

To Ask or Not To Ask: Human-in-the-loop Contextual Bandits with Applications in Robot-Assisted Feeding

Rohan Banerjee¹, Rajat Kumar Jenamani^{*1}, Sidharth Vasudev^{*1},
Amal Nanavati², Sarah Dean^{†1}, Tapomayukh Bhattacharjee^{†1}

Abstract—Robot-assisted bite acquisition involves picking up food items that vary in their shape, compliance, size, and texture. A fully autonomous strategy for bite acquisition is unlikely to efficiently generalize to this wide variety of food items. We propose to leverage the presence of the care recipient to provide feedback when the system encounters novel food items. However, repeatedly asking for help imposes cognitive workload on the user. In this work, we formulate human-in-the-loop bite acquisition within a contextual bandit framework and propose a novel method, LINUCB-QG, that selectively asks for help. This method leverages a predictive model of cognitive workload in response to different types and timings of queries, learned using data from 89 participants collected in an online user study. We demonstrate that this method enhances the balance between task performance and cognitive workload compared to autonomous and querying baselines, through experiments in a food dataset-based simulator and a user study with 18 participants without mobility limitations.

I. INTRODUCTION

Activities of Daily Living (ADLs) [1], such as dressing, bathing, and feeding, are challenging for humans with mobility limitations. These tasks frequently necessitate human caregiver support, which may not always be readily available. Feeding is one example of such an ADL [1], and approximately 1 million people in the U.S. are unable to eat without assistance [2]. Robotic systems have the potential to empower those with mobility limitations to feed themselves, offering a significant step towards independence.

Robot-assisted feeding comprises two major components [3]: bite acquisition [4]–[7], which is the task of picking up a food item, and bite transfer [8, 9], which is the task of transferring it to the mouth of the user. In our work, we focus on bite acquisition, with the goal of learning a policy that can robustly acquire novel food items with varying shapes, colors, textures, compliance, and sizes.

A typical grocery store contains more than 40,000 unique food items [10], motivating the need for bite acquisition strategies that can generalize well to novel food items. Existing state-of-the-art approaches for bite acquisition formulate it as a contextual bandit problem [5, 6], demonstrating that online learning techniques like LINUCB [11] can adapt to unseen food items. However, for certain food items, these methods may require a large number of samples to converge to the optimal acquisition action. Achieving quick adaptation

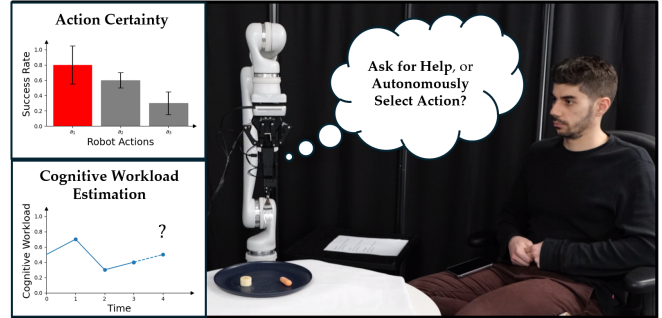


Fig. 1: We present a human-in-the-loop contextual bandit-based framework for robot-assisted bite acquisition and propose a novel method which decides whether to ask for help or autonomously act, by considering both certainty about action performance, and the estimated cognitive workload imposed on the human by querying. It is crucial to avoid damage due to the fragility of food items and to minimize user dissatisfaction due to frequent failures [12]. Yet the significant diversity of food items makes this challenging for fully autonomous strategies.

Our insight is that we can leverage the presence of the care recipient (or their caregiver) to develop online strategies that ask for help to more effectively adapt to novel food items. Incorporating this feedback can give care recipients a sense of agency during eating. While they can potentially provide various types of feedback, such as identifying the food item or indicating where it is located, we assume in our work that the human directly specifies what acquisition action the robot should take for the food item. This approach extends the contextual bandit formulation for bite acquisition to include querying the human-in-the-loop [13]. However, querying too frequently can impose an overwhelming cognitive workload on the user, potentially decreasing technology acceptance [14]. Thus, our key research question is:

How do we balance imposing *minimal cognitive workload* on the user while achieving *maximal bite acquisition success* in a human-in-the-loop contextual bandit framework?

Critical to finding this balance is accurately estimating the cognitive workload placed on a user when they are queried. Existing methods for estimating cognitive workload rely on exteroceptive sensory data, such as physiological and neurological indicators [15]–[17]. However, continuously accessing such sensor data would require users to perpetually wear specialized equipment, which can be invasive. To address this challenge, we develop a non-intrusive data-driven method. We conduct a study with 89 participants without disabilities, gathering data on how various types

^{*}Equal Contribution, [†]Equal Advising.

¹Department of Computer Science, Cornell University {rbb242, rj277, sv355, sdean, tapomayukh}@cornell.edu

²Department of Computer Science and Engineering, University of Washington, Seattle, WA 98195 {amaln}@cs.washington.edu

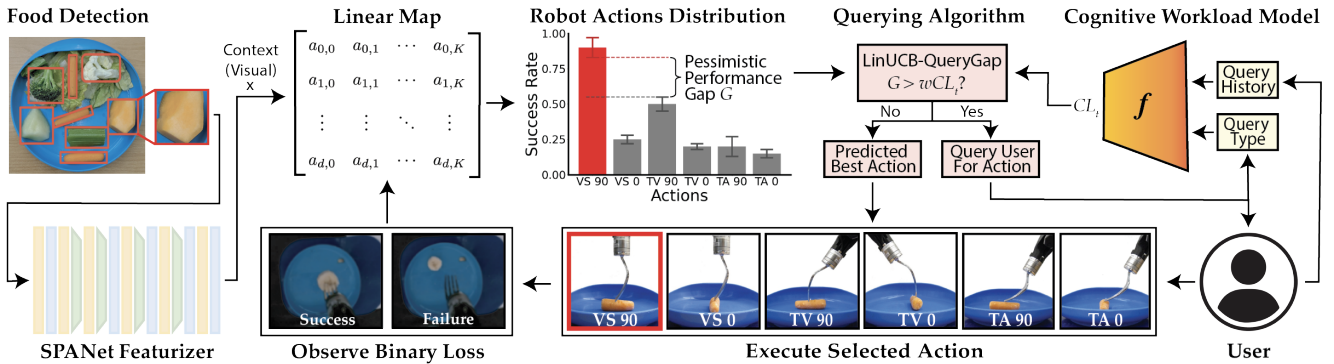


Fig. 2: Human-in-the-loop contextual bandit pipeline for deciding whether to query (a_q) or autonomously select a robot action a_r . Our proposed method, LINUCB-QG, takes into account action uncertainty as measured by the performance gap G between the best and the second best robot action and incorporates a learned cognitive workload model (f) to predict the workload of querying the human CL_t .

of queries related to feeding tasks and the timing of these queries impact the user’s self-reported cognitive load, as measured by the NASA-TLX scale [18]. We tailor the queries in our study to correspond to the most common types of failures encountered in autonomous systems, such as failures due to perception (such as missed detections or misclassification), calibration, or incorrect action selection. The types of queries we solicit from the users range from multiple-choice questions, such as asking the user to identify which of a pair of images corresponds to a particular food item, to open-ended questions that ask the user to either explain why the robot failed to acquire a food item, or even ask the user to suggest an acquisition strategy. From this data, we learn a model capable of predicting the cognitive workload a user may experience in response to a new query, factoring in both the nature of the query and the user’s prior query interactions with the system.

Building on our non-intrusive cognitive workload model, we propose LINUCB-QUERYGAP (LINUCB-QG), a novel algorithm for human-in-the-loop contextual bandits, that decides when to query based on the estimated cognitive workload penalty of the query and the performance uncertainty of candidate actions. We demonstrate through simulated experiments on a dataset of 16 food items [4] that LINUCB-QG achieves a better balance between induced cognitive workload and bite acquisition success for novel food items compared to three baselines: (i) LINUCB [11]: a state-of-the-art fully autonomous baseline, (ii) ALWAYSQUERY: a baseline that always queries, and (iii) LINUCB-EXPDECAY: a naive querying algorithm that does not incorporate our learned cognitive workload model. LINUCB-QG achieves higher task performance compared to LINUCB and LINUCB-EXPDECAY, while imposing lower cognitive workload compared to ALWAYSQUERY and LINUCB-EXPDECAY.

We validate the effectiveness of our proposed method in a real-world robot-assisted feeding user study involving 18 individuals without mobility limitations. Our study uses three different food types that have variable material properties: banana slices, carrots, and cantaloupe. We find that LINUCB-QG achieves a statistically significant improvement of 26% higher task success compared to LINUCB, while also achieving a 47% lower change in cognitive workload compared to ALWAYSQUERY.

Our contributions are as follows:

- We propose a human-in-the-loop contextual bandit framework that incorporates the cognitive workload of querying and apply this to bite acquisition.
- We collect a dataset on how feeding-related queries affect cognitive workload, measured by the NASA-TLX scale.
- We develop a model using this dataset to predict the expected cognitive workload of a prospective query without relying on exteroceptive sensor data.
- We propose a novel method, LINUCB-QG, that leverages our learned cognitive workload model to balance the trade-off between acquisition success and querying frequency.
- We demonstrate LINUCB-QG’s efficacy over a state-of-the-art fully autonomous baseline [11] and various competitive querying baselines through simulated experiments on a dataset of 16 food types and a real-world study with 18 users without mobility limitations.

II. RELATED WORK

We outline prior work in two areas relating to the trade-off between task performance and cognitive workload: (i) algorithms that decide when to ask the human for help, and (ii) measuring and learning to predict cognitive workload (additional work in Appendix).

Human-in-the-loop algorithms. Our problem setting is an instance of learning to defer to an expert [19]. In this setting, an agent must decide whether to produce decisions according to its own learned model, or defer to the decisions from one or more experts, such as oracle models or humans. Most approaches operate in the supervised learning [19]–[22] or RL [23] domains. Motivated by the constraints of robot-assisted bite acquisition, in which we observe independent contexts and receive sparse feedback in response to robot acquisition actions based on those contexts, our work focuses on learning-to-defer policies in an online contextual bandit setting. Most learning-to-defer approaches incorporate a fixed cost of querying the expert [20]–[22], or an imperfect expert [21], while in our work we propose to estimate a time-varying penalty for deferral using a data-driven model.

Another set of human-in-the-loop papers explore active learning algorithms for robotics domains [24]–[26], in which the robotic agent must decide which instances to query for [25, 26], or which of multiple types of feedback to solicit from the expert [24]. While some of these algorithms

incorporate the balance between task performance and the human cost of querying, our work again differs in that we use a data-driven model of querying cost, and in our application to the challenging manipulation task of bite acquisition.

Cognitive workload modeling. Our human-in-the-loop algorithms need to monitor and predict the cognitive workload of asking for help to ensure the workload on the user is not excessive. Most literature in the space of measuring cognitive workload focuses on measuring neurological or physiological signals such as EEG [15], ECG/EDA [27] or pupil position or diameter [17, 28]. These approaches then train a supervised model that learns to predict cognitive workload based on these signals. The challenge in using such models is that measuring the physiological signals requires physical infrastructure that can be costly and require specialized equipment. Cognitive workload can also be estimated post-hoc using subjective metrics, such as with the NASA-TLX survey [15]. In contrast to works that use specialized sensors, we develop a data-driven predictive model of cognitive workload trained on self-reported NASA-TLX survey results. This model can estimate the expected cognitive workload of a query given the interaction history, timing and type of the query.

III. PROBLEM FORMULATION

We use an online learning formulation based on the contextual bandit approach used in state-of-the-art bite acquisition literature [5, 6]. In the contextual bandit setting [11], the learner receives a context x_t (corresponding to a food item) at each timestep, and must select actions $a_t \in \mathcal{A}$ that minimize regret over a fixed time horizon T , given by:

$$\sum_{t=1}^T \mathbb{E}[r_t | x_t, a_t^*, t] - \sum_{t=1}^T \mathbb{E}[r_t | x_t, a_t, t]$$

where r_t denotes the scalar reward received by the learner, $a_t^* \triangleq a^*(x_t)$ denotes the optimal action (i.e. the action that maximizes the reward r_t) at time t given context x_t , and the expectations are taken over the stochasticity in r_t .

The two primary components of contextual bandit algorithms are policy updating (how to update the policy based on reward observations) and action selection (how to sample actions during the learning process) [29]. For policy updating, we use parameterized reward models that are learned by regression, although we note that our algorithms work more generally for any optimism-based contextual bandit sub-routine. Our primary focus is on action selection, where in our setting the learner chooses between selecting a robot action and an action for querying the human.

In our problem setting, we assume that we have access to a dataset D collected from a robotic manipulator, consisting of raw observations $o \in \mathcal{O}$, actions $a \in \mathcal{A}$, and observed binary rewards r . We use D to pretrain and validate our contextual bandit algorithms, but our algorithms also apply to the fully online setting without *a priori* access to D . The dataset D and contextual bandit setting are characterized as follows:

- **Observation space** \mathcal{O} : RGB images containing a single bite-sized food item on a plate (sampled from a set of 16

distinct food types). The food item is either isolated, close to the plate edge, or on top of another food item [4].

- **Action space** \mathcal{A} : A discrete action space consisting of 7 actions in total - 6 robot actions a_r for $r \in \{1, \dots, 6\}$ shown in Figure 2 (bottom), and 1 query action a_q . Each robot action is a pair consisting of one of three pitch configurations (tilted angled (TA), vertical skewer (VS), tilted vertical (TV)) and one of two roll configurations (0° , 90°), relative to the orientation of the food [4, 30].
- **Context space** \mathcal{X} : As in [5], we derive a lower-dimensional context x from the visual observations o using the SPANet network [4]. A critical assumption for our bandit algorithms is the realizability of a linear relationship between the context x and the expected reward $\mathbb{E}[r]$. SPANet is pretrained in a fully-supervised manner to predict $s_o(o, a)$, the probability that action a succeeds for observation o . Because the final layer of SPANet is linear, we use the penultimate activations of SPANet as our context, with dimensionality $d = 2048$.

In our setup, if the learner selects one of the robot actions a_r , it receives an observed binary reward corresponding to whether the action was successful for context x_t . If the learner instead selects the query action a_q , it first receives expert feedback from the human in the form of the optimal robot action $a^*(x_t)$ that has the highest probability of successfully picking up the food item contained in x_t . It then executes the robot action a_t^* and receives the binary reward corresponding to the success of this action. However, the act of querying the human also imposes a cognitive workload penalty on the learner, given by the human’s latent cognitive workload state at time t , which we denote as CL_t .

In order to incorporate both robot action success and cognitive workload into our bandit formulation, we model the total time-dependent expected reward $\mathbb{E}[r_t | x_t, a_t, t]$ as composed of two components: (1) the expected task reward $r_{task}(x_t, a_t)$, which is the probability that action a_t succeeds for food context x_t , (2) the expected cognitive workload reward $r_{CL}(x_t, a_t, t)$ associated with selecting query actions a_q . We define $\mathbb{E}[r_t | x_t, a_t, t]$ as follows:

$$\mathbb{E}[r_t | x_t, a_t, t] \triangleq w_{task} r_{task}(x_t, a_t) + w_{CL} r_{CL}(x_t, a_t, t)$$

where w_{task} and w_{CL} are positive, scalar weights that sum to 1. Our goal is to learn a policy $\pi(a | x, t)$ that maximizes $\sum_{t=1}^T \mathbb{E}[r_t | x_t, a_t, t]$ over any sequence of food items over T timesteps.

More formally, the expected task reward depends on $s_x(x, a)$, the probability that action a succeeds for context x . We define $r_{task}(x_t, a_t)$ to be $s_x(x_t, a_t)$ if a_t is a robot action a_r , and $s_x(x_t, a^*(x_t))$ if a_t is the query action a_q . Similarly, we define $r_{CL}(x_t, a_t, t)$ to be 0 if a_t is a robot action a_r , and $-CL_t$ if a_t is the query action a_q . The expected task reward $r_{task}(x_t, a_t)$, which is a probability value, can be understood as the mean of a Bernoulli random variable. The observed task rewards r in the dataset D can be thought of as samples from the associated Bernoulli distribution.

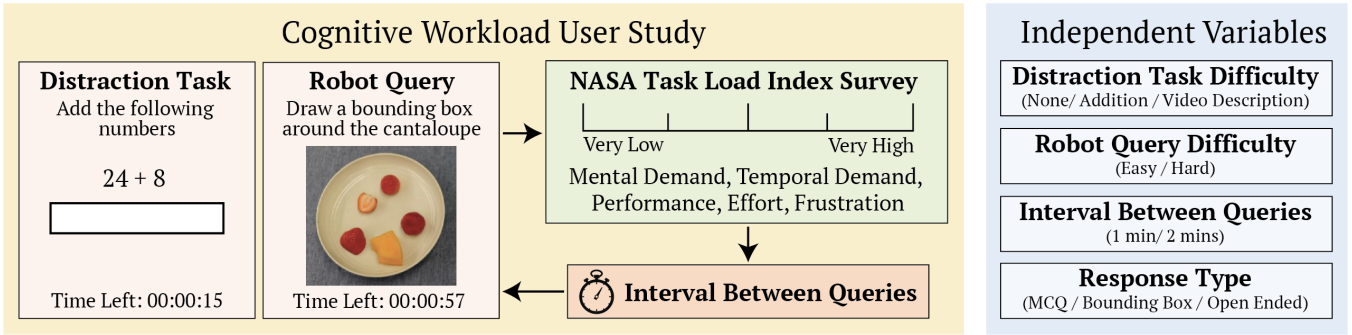


Fig. 3: *Left*: Cognitive workload user study setup, illustrating the format of the distraction task and robot query task, and the NASA-TLX survey recorded after every robot query. *Right*: Independent variables that can affect user’s cognitive workload varied during the study.

IV. COGNITIVE WORKLOAD MODELING

Our proposed human-in-the-loop contextual bandit algorithms rely on estimation of the cognitive workload state CL_t defined in Section III. We estimate CL_t by first designing a user study to understand how cognitive workload responds to requests for help, which we describe in IV-A. We then learn a parameterized predictive model of cognitive workload using this user study data, which we describe in IV-B.

A. Cognitive Workload User Study

While we focus on direct human action feedback in our work, our user study design encompasses other types of human intervention as shown in Figure 3. In a robotic caregiving scenario, a feeding system may require various types of help from the end-user (or caregiver) for successful bite acquisition. For example, the system may ask for semantic labels of food items, or to draw a bounding box around a food item (if perception is inaccurate). The system may even ask an open-ended question on why an acquisition attempt failed. The requested response type may have a varying impact on cognitive workload [13, 31]. For instance, a semantic label response may impose less workload than an open-ended response. In addition, the end-user of the system and the caregiver may simultaneously be busy with other tasks, such as watching TV while eating. We conduct an online user study that captures the above factors to determine how an individual’s cognitive workload changes in response to requests for assistance from an autonomous system.

In the user study, participants complete a distraction task while the “robot” periodically interrupts them with a query for help. The distraction task is meant to artificially vary user busyness to mirror realistic robotic caregiving scenarios. The robot queries are based on realistic forms of assistance that a feeding system may require during bite acquisition.

In this study, we vary four independent variables that we hypothesize impact the user’s cognitive workload:

- 1) Robot query difficulty (d_t): 2 options - easy or hard.
- 2) Distraction task difficulty ($dist_t$): 3 options - no distraction task, an easy numeric addition task, or a hard video transcription task.
- 3) The time interval between successive robot queries (ΔT): 2 options - either 1 minute or 2 minutes.
- 4) Response type ($resp_t$): 3 options - (a) a multiple-choice question (MCQ) asking for a semantic label, (b) asking

the user to draw a bounding box (BB) around a food item, or (c) an open-ended (OE) question asking the user to explain why an acquisition attempt failed.

Each participant sees 12 distinct study conditions, one for each of the 2 settings of d_t , 3 settings of $dist_t$, and 2 settings of ΔT . During each study condition, the user is presented with distraction tasks on the left side of their screen, along with a sequence of robot queries (with varying response types $resp_t$) on the right side of their screen, as shown in Figure 3. Each user sees the same set of robot queries for a particular study condition, but the ordering of these questions is random for a particular user. We structure each study condition to last for a total of 5.5 minutes to allow for a variable number of robot queries, with the entire study taking roughly 1.5 hr.

We measure the users’ self-reported cognitive workload (the dependent variable in our study) after every robot query within a study condition, and also at the end of each study condition. We measure cognitive workload with 5 NASA-TLX [18, 32] subscales (mental, temporal, performance, effort, frustration)¹, each measured on a 5-point Likert scale.

In total, we collect data for 89 users (40 male, 49 female; ages 19-68). This study was approved by the Institutional Review Board at Cornell University (#IRB0147183).

B. Cognitive Workload Predictive Model

We learn a predictive model of cognitive workload using the data collected from the user study described in Section IV-A. We consider a set of cognitive workload models that operate in discrete time. That is, the time variable t refers to an integer number of timesteps since the beginning of a condition, where each timestep corresponds to a fixed time spacing Δt (set to 10s in our experiments).

The model has the form $CL_t = f(CL_0, Q_t; \theta)$, where CL_0 is the initial workload at the beginning of a condition, $Q_t = \{(d_{t'}, resp_{t'}, dist_{t'})\}_{t'=1}^t$ is the history of previous queries (where d_t , $resp_t$, and $dist_t$ are the query variables defined in Section IV-A), and θ are the model parameters. We convert the raw NASA-TLX score into a single scalar in $[0, 1]$ by normalizing and taking a weighted average of the 5 subscales (weight details in Appendix).

Linear discrete-time models. Our goal is to select the simplest model class that could capture a dependency be-

¹We eliminate the “physical effort” subscale since the study is conducted online on users without disabilities.

tween the current workload and the query history Q_t . We therefore choose to define a linear predictive workload model, which is both easily learnable using least-squares regression and has interpretable parameters θ . More specifically, we use the following linear predictive model, inspired by Granger models from the causality literature [33, 34]:

$$CL_t = \gamma CL_0 + \sum_{i=0}^{H-1} \mathbf{w}_i^T [d_{t-i}, resp_{t-i}, dist_{t-i}] + w_0$$

where \mathbf{w}_i represents the effect of the query asked i timesteps in the past on the workload at the current time t , H represents the history length of the model, and w_0 is a bias term. We learn the parameters of the above model using linear regression, where we convert d_t , $resp_t$, and $dist_t$ into features using one-hot encodings, and generate a training pair for each robot task query in our study. We zero-pad the query variables $[d_{t-i}, resp_{t-i}, dist_{t-i}]$ if there are no queries in the discrete time window $t - i$, or if we run out of history.

For our real-world user study, we use a Granger model with $H = 5$ and a ridge constraint on the parameters, achieving a cross-validation mean test MSE of 0.0573 ± 0.0127 on the full cognitive workload dataset. Please refer to the Appendix for further discussion about model selection, along with cross-validation performance values for other models (including models with different values of H and different regularization constraints on the model parameters).

V. HUMAN-IN-THE-LOOP ALGORITHMS

In the previous section, we described models that learn to predict the user’s cognitive workload state CL_t given their query history and the current query type. These learned workload models can allow a decision-making algorithm to predict the cognitive workload CL_t associated with asking for help. We now outline a set of algorithms that decide whether to ask for help or whether to act autonomously. Specifically, we consider four human-in-the-loop contextual bandit algorithms: one fully autonomous algorithm, and three algorithms that can ask for help from the human.

Fully autonomous algorithm. Our fully autonomous baseline is LinUCB [11], which is the state-of-the-art algorithm for acquisition of unseen bite-sized food items such as banana and apple slices [5, 6]. LinUCB selects the action for an observed context x that maximizes an upper-confidence bound (UCB) estimate of the reward for each possible robot action, given by $UCB_{a_r} = \theta_{a_r}^T x + \alpha b_{a_r}$. Here, θ_{a_r} is the parameter vector for a linear reward model that is learned through regression on a context matrix X_{a_r} and observed rewards for each action a_r , where X_{a_r} includes the contexts seen for robot action a_r during pretraining and online validation, $\alpha > 0$ is a parameter that corresponds to a particular confidence level in the accuracy of the UCB estimate, and $b_{a_r} = (x^T (X_{a_r}^T X_{a_r} + \lambda I)^{-1} x)^{1/2}$ is the UCB bonus with L_2 regularization given by parameter λ . The size of the reward confidence interval αb_{a_r} reflects the uncertainty in the algorithm’s knowledge about the true reward for the given context-action pair.

Algorithm 1 LINUCB-QG.

- 1: Inputs: Context x , scaling factor w , time t , initial workload CL_0 , workload model f , model parameters θ
 - 2: For all robot actions a_r , compute UCB bonus b_{a_r} and UCB value UCB_{a_r} .
 - 3: Let $a^* = \arg \max_{a_r} \theta_{a_r}^T x$, $a^- = \arg \max_{a_r \neq a^*} \theta_{a_r}^T x$
 - 4: Define $G \triangleq (\theta_{a^-}^T x + \alpha b_{a^-}) - (\theta_{a^*}^T x - \alpha b_{a^*})$
 - 5: Set $a = \begin{cases} a_q & \text{if } G > wf(CL_0, Q_t; \theta) \\ \arg \max_{a_r} UCB_{a_r} & \text{otherwise} \end{cases}$
 - 6: **return** a
-

Querying algorithms. We consider the following three querying algorithms, where all algorithms decide to query the human or select the robot action that maximizes UCB_{a_r} .

- 1) ALWAYSQUERY, which always queries the user.
- 2) LINUCB-EXPDECAY, which queries with an exponentially-decaying probability (characterized by decay rate c) that is a function of the number of food items seen within an episode (detailed algorithm formulation in Appendix).
- 3) LINUCB-QUERY-GAP (LINUCB-QG), which is defined in Algorithm 1. LINUCB-QG decides to query if the worst-case performance gap between the best action a^* and second-best action a^- exceeds the predicted workload penalty, with scaling factor w .

In LINUCB-QG, the worst-case gap is the difference between a pessimistic estimate of the reward of a^* and an optimistic estimate of the reward of a^- , associated with the confidence intervals of each action. This gap is illustrated in Figure 2 (top). A larger gap represents a greater risk that the predicted best arm may be suboptimal, increasing the odds that the reward gain from querying will be greater than CL_t . Therefore, querying only when the gap is sufficiently large is likely to improve the tradeoff between task reward and cognitive workload.

We define the predicted workload penalty to be the counterfactual cognitive workload CL_t if we were to query at the current time. To estimate the predicted workload, we invoke the learned workload model $CL_t = f(CL_0, Q_t; \theta)$, where when constructing Q_t , we set the query type variables to be $d_t = \text{easy}$, $resp_t = \text{MCQ}$, $dist_t = \text{“no distraction task”}$ for all t where the selected action $a_t = a_q$.

VI. EVALUATION + RESULTS

We evaluate the performance of our human-in-the-loop contextual bandit algorithms using two setups: (i) a simulation testbed (Section VI-A), and (ii) a real world user study with human subjects without disabilities (Section VI-B).

Before diving into our experimental settings, we make one remark about our evaluation of the contextual bandit algorithms. Recall that the expected reward $\mathbb{E}[r_t | x_t, a_t, t]$ defined in Section III depends explicitly on the cognitive workload CL_t for all times t for which $a_t = a_q$. However, measuring the intermediate workload values after every query would require administering a survey after each query, which is impractical in the real world. Therefore, in our experimental

Method	$r_{task,avg}$	ΔCL	M_{wt}	f_q	t_{conv}
LINUCB	0.289 ± 0.101	-0.5 ± 0	0.415 ± 0.040	-	3.92 ± 1.342
ALWAYSQUERY	0.638 ± 0.189	-0.329 ± 0.106	0.453 ± 0.042	1 ± 0	1.68 ± 0.392
LINUCB-EXPDECAY	0.368 ± 0.135	-0.496 ± 0.014	0.445 ± 0.050	0.4 ± 0.219	2.94 ± 0.894
LINUCB-QG	0.407 ± 0.059	-0.5 ± 0	0.463 ± 0.024	0.76 ± 0.08	2.52 ± 0.449

TABLE I: Querying bandit algorithm metrics in simulation on the test set, corresponding to $w_{task} = 0.4$. Averages are across 5 random seeds (For LINUCB-EXPDECAY, we also average across 5 policy random seeds). Values for $r_{task,avg}$ and r_{CL} correspond to the hyperparameter setting with maximal M_{wt} on the validation set.

formulation in both simulation and in the real study, we will assume that we cannot observe the intermediate workload values, but we instead observe only the initial and final workload values. We therefore evaluate our algorithms on the following surrogate objective:

$$w_{task} \left[\frac{1}{T} \sum_{t=1}^T r_{task}(x_t, a_t) \right] - w_{CL}(CL_T - CL_0)$$

In the above expression, CL_0 and CL_T are the initial and final workload, where $CL_T = f(CL_0, Q_T; \theta)$.

A. Simulated Testbed

We first create a simulation testbed based on the food dataset from [4], which contains food images collected from a real Kinova Gen-2 robot arm [35] instrumented with an RGB-D camera on the end effector. A plate containing bite-sized food was located in front of the robot arm. The dataset contains 16 distinct food types, where for each food type we have 30 trials for each of the 6 robot actions a_r . Each trial contains observation data $o \in \mathcal{O}$, along with action data $a \in \mathcal{A}$ and binary observed task rewards r .

The simulation environment mimics the food interaction that would be expected in the real world as follows. Before any policy interaction, we calculate estimates of the expected success probability $s_x(x, a_r)$ for each food type and action by taking the empirical mean of successes in the dataset. For a given food type, we first draw a random image of that food type from the dataset. We then generate the context x for that image by passing the image through the SPANet network.

When the bandit policy selects a robot action a_r , the simulator produces a binary observed task reward r by sampling from a Bernoulli distribution whose success probability is the precomputed estimate of $s_x(x, a_r)$. If this reward r is equal to 1 (i.e. the action a succeeded for food context x), the simulator declares that the bandit has converged, and then produces a new food type at the next timestep. If r is equal to 0, we simulate observing the same food type at the next timestep by drawing a new random image of the same food type from the dataset. We draw a new image because acquisition actions in the real world alter the physical state of food items, changing their visual appearance. We repeat the above process until we exceed the maximum number of attempts N_{att} for that food item, which we set to 10 in our simulated experiments.

When the bandit policy selects a query action a_q , the expert robot action $a^*(x)$ can sometimes fail due to variability in the material properties of the food item. If the observed reward r is 0 for this expert action, the bandit policy will repeatedly execute the action until either convergence

is achieved, or the maximum number of attempts N_{att} is reached. This is because the policy already knows the optimal action for the current food item once it has queried.

Metrics. For each algorithm, we compute a set of 5 objective metrics to evaluate the tradeoff between task performance and cognitive workload. We compute the mean episodic task reward $r_{task,avg} = \frac{1}{T} \sum_{t=1}^T r_{task}(x_t, a_t)$, which measures the efficiency of successful food acquisition. We also compute the episodic change in cognitive workload $\Delta CL = CL_T - CL_0$. We compute our surrogate objective $M_{wt} = w_{task} r_{task,avg} - w_{CL} \Delta CL$, where w_{task} and w_{CL} represent user-specific preferences for the task performance/cognitive workload tradeoff. We additionally report the number of timesteps taken to converge t_{conv} , which provides additional insights into task performance, and the fraction of food items for which we queried f_q , which provides an insight into cognitive workload.

Evaluating cognitive workload in simulation. In our simulation environment, we use the learned cognitive workload model f both for action-selection (in the case of LINUCB-QG), and for the computation of the evaluation metrics ΔCL and M_{wt} . During the rollout of a particular bandit policy, we evolve the workload model state CL_t according to the learned model whenever we query. For all experiments in this section, we use a Granger model with history length $H = 10$ (details in the Appendix). We set $CL_0 = 0.5$ for all experiments, corresponding to a median user’s initial workload.

Pretrain, validation, and test sets. In our experiments, we partition the full set of 16 food types into a pretraining set (which is used to train the SPANet featurizer), a validation set (which is used to tune the decay rate c for LINUCB-EXPDECAY and the scaling factor w for LINUCB-QG), and a test set (used to evaluate the aforementioned metrics). We choose our validation and test sets to include food items with varying material properties, where our validation set contains cantaloupe and grape, while our test set contains banana and carrot. Our pretrain set contains the remaining 10 food types in the food dataset. For a particular setting of (w_{task}, w_{cl}) , we use the validation set to select the hyperparameter that maximizes the weighted metric M_{wt} .

Results. We investigate how LINUCB-QG balances the tradeoff between task reward and cognitive workload. Table I compares the four algorithms using the previously-described metrics, for the setting where $w_{task} = 0.4$. This setting corresponds to an intermediate preference between task performance and cognitive workload, with a slight preference for minimizing workload over maximizing task reward.

We note that LINUCB-QG has a lower mean ΔCL value

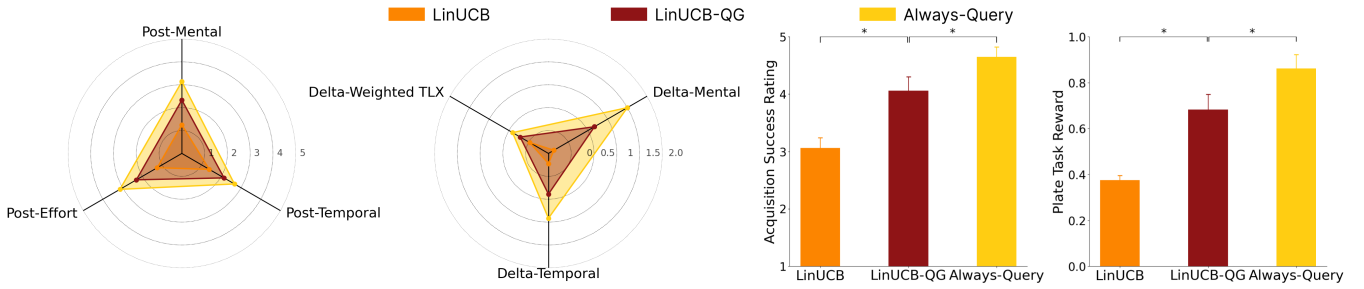


Fig. 4: Real-world user study results. *Left*: LINUCB-QG significantly reduces cognitive workload compared to ALWAYS-QUERY as shown by three post-method metrics and three changes in workload metrics. *Right*: LINUCB-QG significantly outperforms LINUCB in bite acquisition success, as demonstrated by both subjective and objective success metrics. Error bars indicate standard error.

compared to ALWAYS-QUERY and LINUCB-EXPDECAY. Additionally, LINUCB-QG has higher average task reward $r_{task,avg}$ than LINUCB and LINUCB-EXPDECAY. Finally, we note that LINUCB-QG has a higher mean weighted metric M_{wt} than all of the other methods. Overall, this suggests that LINUCB-QG achieves the best tradeoff between task reward and cognitive workload out of the four methods that we consider (additional results in the Appendix).

B. Real-World User Study

To evaluate the effectiveness of LINUCB-QG in trading off task performance with cognitive workload in the real world, we conduct a user study including 18 users (8 male, 10 female; ages 19-31) without mobility limitations. Of all the participants, 66% had previous experience working or interacting with robots. We investigate whether LINUCB-QG would achieve improved task performance compared to the non-querying LINUCB baseline, while still minimizing cognitive workload compared to the ALWAYS-QUERY baseline. This study was approved by the Institutional Review Board at Cornell University (Protocol #IRB0010477).

Study setup. We use a Kinova Gen-3 6-DoF robot arm with a Robotiq 2F-85 gripper, equipped with a custom feeding tool (details in Appendix). For each method, we present the user with a plate of 3 food items (banana, carrot, and cantaloupe). We give each method a fixed maximum number of acquisition attempts, set to 3 attempts to ensure a reasonable study duration. In the scenario where a human is queried, they provide feedback using a speech-to-text interface. Users evaluate each of the three methods in sequence in a counterbalanced order. We measure the cognitive workload before and after each method by asking a series of questions covering 4 of the 5 NASA-TLX subscales: mental, temporal, performance, and effort (exact question wording in Appendix). For each user, we conduct 2 repetitions of the 3 food items for all 3 methods, for a total of 18 food trials.

We select cantaloupe, carrot and banana because they embody diverse characteristics salient for acquisition, such as shape and compliance, and offer unique challenges: cantaloupe can be acquired with any of the six robot actions; carrots, being hard and thin, necessitate actions that can apply sufficient penetration force and have fork tines perpendicular to food major axis (TV90 and VS90); bananas are soft, requiring the tilted-angled actions (TA0 and TA90) [5].

Metrics. We define a set of 7 subjective and 3 objective metrics to compare the 3 methods. 4 subjective metrics

directly correspond to the NASA TLX subscale measurements that we ask after each method, and are denoted Post-Mental, Post-Temporal, Post-Performance, and Post-Effort. The other 3 subjective metrics correspond to changes in the workload over the duration of each method: Delta-Mental (the change in mental subscale), Delta-Temporal (the change in temporal subscale), and Delta-Weighted TLX (the change in weighted TLX score, using the weighting function described in the Appendix). The 3 objective metrics are the mean episodic task reward per plate ($r_{task,avg}$), the mean number of successes per plate ($n_{success}$), and the mean number of timesteps in which we query (n_q).

Results. Overall, we find that out of the three methods, LINUCB-QG is the most balanced approach to human-in-the-loop bite acquisition. It is more efficient than LINUCB, and also achieves improved cognitive load compared to ALWAYS-QUERY. LINUCB is typically able to pick up the carrot or cantaloupe after 1-2 timesteps, but is almost never able to pick up the banana within 3 timesteps. In contrast, ALWAYS-QUERY always queries the user for the optimal action and thus successfully picks up the food in the first time-step, but at the expense of imposing higher cognitive workload on the user. Our method, LINUCB-QG, asks the human for help for the banana and autonomously acts for the carrot and cantaloupe in most trials, balancing task performance with cognitive workload.

1) *Task success results:* Figure 4 (right) compares the task success of the three methods in our study, based on the subjective Post-Performance metric and the objective mean episodic task reward metric. We find that LINUCB-QG has higher objective success ratings (not only for the mean episodic metric, but for all objective metrics) and a higher subjective success rating compared to LINUCB. Overall, LINUCB-QG is more efficient than LINUCB.

2) *Cognitive workload results:* Figure 4 (left) illustrates the results for subjective cognitive workload. The left figure includes 3 of the 4 post-method metrics, while the right figure includes the 3 metrics corresponding to change in workload. We found that LINUCB-QG has lower subjective cognitive workload scores (for the mental, temporal, and effort subscales) compared to ALWAYS-QUERY. This suggests that the selective querying behavior of LINUCB-QG imposes a lower cognitive workload compared to the frequent, deterministic querying behavior of ALWAYS-QUERY.

All results are statistically significant as assessed using

the Wilcoxon paired signed-rank test with significance level $\alpha = 0.05$. Full comparisons of the three methods across all metrics are contained in the Appendix.

VII. DISCUSSION

We propose LINUCB-QG, a human-in-the-loop contextual bandit method that leverages a learned user cognitive workload model to balance task performance with user cognitive workload. We demonstrate that our method outperforms state-of-the-art baselines in bite acquisition through experiments in a simulated setting and in a real-world user study with individuals without mobility limitations.

A limitation of this work is the absence of participants with mobility limitations in our real-world user study. This leaves the exploration of our method's usability for individuals with mobility limitations as an area for future research. Furthermore, future explorations could benefit from incorporating different types of queries in the real-robot study, beyond just the best acquisition action. Another promising direction would be to explore predictive models that account for objective measurements of cognitive workload and have task-relevant inductive biases.

REFERENCES

- [1] S. Katz, A. B. Ford, R. W. Moskowitz, B. A. Jackson, and M. W. Jaffe, "Studies of illness in the aged: The index of adl: A standardized measure of biological and psychosocial function," *Jama*, vol. 185, no. 12, pp. 914–919, 1963.
- [2] M. W. Brault, "Americans with disabilities: 2010," *Current population reports*, vol. 7, pp. 70–131, 2012.
- [3] R. Madan, R. K. Jenamani, V. T. Nguyen, et al., "Sparcs: Structuring physically assistive robotics for caregiving with stakeholders-in-the-loop," in *2022 IEEE/RSJ International Conference on Intelligent Robots and Systems (IROS)*, IEEE, 2022, pp. 641–648.
- [4] R. Feng, Y. Kim, G. Lee, et al., "Robot-assisted feeding: Generalizing skewering strategies across food items on a plate," in *The International Symposium of Robotics Research*, Springer, 2019, pp. 427–442.
- [5] E. K. Gordon, X. Meng, T. Bhattacharjee, M. Barnes, and S. S. Srinivasa, "Adaptive robot-assisted feeding: An online learning framework for acquiring previously unseen food items," in *2020 IEEE/RSJ International Conference on Intelligent Robots and Systems (IROS)*, IEEE, 2020, pp. 9659–9666.
- [6] E. K. Gordon, S. Roychowdhury, T. Bhattacharjee, K. Jamieson, and S. S. Srinivasa, "Leveraging post hoc context for faster learning in bandit settings with applications in robot-assisted feeding," in *2021 IEEE International Conference on Robotics and Automation (ICRA)*, IEEE, 2021, pp. 10528–10535.
- [7] P. Sundaresan, S. Belkhale, and D. Sadigh, "Learning visuo-haptic skewering strategies for robot-assisted feeding," in *6th Annual Conference on Robot Learning*, 2022.
- [8] D. Gallenberger, T. Bhattacharjee, Y. Kim, and S. S. Srinivasa, "Transfer depends on acquisition: Analyzing manipulation strategies for robotic feeding," in *2019 14th ACM/IEEE International Conference on Human-Robot Interaction (HRI)*, IEEE, 2019, pp. 267–276.
- [9] S. Belkhale, E. K. Gordon, Y. Chen, S. Srinivasa, T. Bhattacharjee, and D. Sadigh, "Balancing efficiency and comfort in robot-assisted bite transfer," in *2022 International Conference on Robotics and Automation (ICRA)*, IEEE, 2022, pp. 4757–4763.
- [10] A. Malito, "Grocery stores carry 40,000 more items than they did in the 1990s," *MarketWatch*, June, vol. 17, 2017.
- [11] L. Li, W. Chu, J. Langford, and R. E. Schapire, "A contextual-bandit approach to personalized news article recommendation," in *Proceedings of the 19th international conference on World wide web*, 2010, pp. 661–670.
- [12] T. Bhattacharjee, E. K. Gordon, R. Scalise, et al., "Is more autonomy always better? exploring preferences of users with mobility impairments in robot-assisted feeding," in *Proceedings of the 2020 ACM/IEEE international conference on human-robot interaction*, 2020, pp. 181–190.
- [13] Y. Cui, P. Koppol, H. Admoni, et al., "Understanding the relationship between interactions and outcomes in human-in-the-loop machine learning," in *International Joint Conference on Artificial Intelligence*, 2021.
- [14] T. Fong, C. Thorpe, and C. Baur, "Robot, asker of questions," *Robotics and Autonomous systems*, vol. 42, no. 3-4, pp. 235–243, 2003.
- [15] S. Shayesteh and H. Jebelli, "Investigating the impact of construction robots autonomy level on workers' cognitive load," in *Canadian Society of Civil Engineering Annual Conference*, Springer, 2021, pp. 255–267.
- [16] A. Aygun, T. Nguyen, Z. Haga, S. Aeron, and M. Scheutz, "Investigating methods for cognitive workload estimation for assistive robots," *Sensors*, 2022.
- [17] L. Fridman, B. Reimer, B. Mehler, and W. T. Freeman, "Cognitive load estimation in the wild," in *Proceedings of the 2018 chi conference on human factors in computing systems*, 2018, pp. 1–9.
- [18] S. G. Hart and L. E. Staveland, "Development of nasa-tlx (task load index): Results of empirical and theoretical research," in *Advances in psychology*, vol. 52, Elsevier, 1988, pp. 139–183.
- [19] M. Raghu, K. Blumer, G. Corrado, J. Kleinberg, Z. Obermeyer, and S. Mullainathan, "The algorithmic automation problem: Prediction, triage, and human effort," *arXiv preprint arXiv:1903.12220*, 2019.
- [20] V. Keswani, M. Lease, and K. Kenthapadi, "Towards unbiased and accurate deferral to multiple experts," in *Proceedings of the 2021 AAAI/ACM Conference on AI, Ethics, and Society*, 2021, pp. 154–165.
- [21] H. Narasimhan, W. Jitkrittum, A. K. Menon, A. Rawat, and S. Kumar, "Post-hoc estimators for learning to defer to an expert," *Advances in Neural Information Processing Systems*, vol. 35, pp. 29292–29304, 2022.
- [22] H. Mozannar and D. Sontag, "Consistent estimators for learning to defer to an expert," in *International Conference on Machine Learning*, PMLR, 2020, pp. 7076–7087.
- [23] S. Joshi, S. Parbhoo, and F. Doshi-Velez, "Learning-to-defer for sequential medical decision-making under uncertainty," *arXiv preprint arXiv:2109.06312*, 2021.
- [24] T. Fitzgerald, P. Koppol, P. Callaghan, et al., "Inquire: Interactive querying for user-aware informative reasoning," in *6th Annual Conference on Robot Learning*, 2022.
- [25] M. Racca, A. Oulasvirta, and V. Kyrki, "Teacher-aware active robot learning," in *2019 14th ACM/IEEE International Conference on Human-Robot Interaction (HRI)*, IEEE, 2019, pp. 335–343.
- [26] A. Li and T. Silver, "Embodied active learning of relational state abstractions for bilevel planning," *arXiv preprint arXiv:2303.04912*, 2023.
- [27] A. Rajavenkatanarayanan, H. R. Nambiappan, M. Kyrarini, and F. Makedon, "Towards a real-time cognitive load assessment system for industrial human-robot cooperation," in *2020 29th IEEE International Conference on Robot and Human Interactive Communication (RO-MAN)*, IEEE, 2020, pp. 698–705.
- [28] M. I. Ahmad, J. Bernotat, K. Lohan, and F. Eyssele, "Trust and cognitive load during human-robot interaction," *arXiv preprint arXiv:1909.05160*, 2019.
- [29] T. Lattimore and C. Szepesvári, *Bandit algorithms*. Cambridge University Press, 2020.
- [30] T. Bhattacharjee, G. Lee, H. Song, and S. S. Srinivasa, "Towards robotic feeding: Role of haptics in fork-based food manipulation," *IEEE Robotics and Automation Letters*, vol. 4, no. 2, pp. 1485–1492, 2019.
- [31] P. Koppol, H. Admoni, and R. G. Simmons, "Interaction considerations in learning from humans," in *IJCAI*, 2021, pp. 283–291.
- [32] M. Hertzum, "Reference values and subscale patterns for the task load index (tlx): A meta-analytic review," *Ergonomics*, vol. 64, no. 7, pp. 869–878, 2021.
- [33] C. W. Granger, "Investigating causal relations by econometric models and cross-spectral methods," *Econometrica: journal of the Econometric Society*, pp. 424–438, 1969.
- [34] T. Liang and B. Recht, "Randomization inference when n equals one," *arXiv preprint arXiv:2310.16989*, 2023.

- [35] *Kinova robotics*, <https://www.kinovarobotics.com/>, Accessed: 2024-03-17.
- [36] M. Selvaggio, M. Cagnetti, S. Nikolaidis, S. Ivaldi, and B. Siciliano, "Autonomy in physical human-robot interaction: A brief survey," *IEEE Robotics and Automation Letters*, vol. 6, no. 4, pp. 7989–7996, 2021.
- [37] S. Nikolaidis, Y. X. Zhu, D. Hsu, and S. Srinivasa, "Human-robot mutual adaptation in shared autonomy," in *Proceedings of the 2017 ACM/IEEE International Conference on Human-Robot Interaction*, 2017, pp. 294–302.
- [38] S. Jain and B. Argall, "Probabilistic human intent recognition for shared autonomy in assistive robotics," *ACM Transactions on Human-Robot Interaction (THRI)*, vol. 9, no. 1, pp. 1–23, 2019.
- [39] A. Pichler, S. C. Akkaladevi, M. Ikeda, *et al.*, "Towards shared autonomy for robotic tasks in manufacturing," *Procedia Manufacturing*, vol. 11, pp. 72–82, 2017.
- [40] R. K. Jenamani, P. Sundaresan, M. Sakr, T. Bhattacharjee, and D. Sadigh, *Flair: Feeding via long-horizon acquisition of realistic dishes*, Under submission to *Robotics: Science and Systems (RSS)* 2024.

APPENDIX

A. Additional Related Work: Shared Autonomy

A number of papers explore another domain within human-in-the-loop learning referred to as shared autonomy [36]. In this problem setting, the policies of a robotic agent and human user are combined to influence decision-making for a particular task. Shared autonomy approaches differ in the types of information that they infer about the human, such as the goals of the human [37, 38], and also in the degree to which human input guides the autonomous system [39]. Our work differs in that our approach selects an action from either the agent or the human without blending the two, and we incorporate a human cognitive workload model distinct from human intent.

B. NASA-TLX weighting function.

Throughout the paper, we define the cognitive workload state CL to be the following weighted sum of the raw NASA-TLX subscales: $CL = 0.4 \cdot \text{mental} + 0.2 \cdot \text{temporal} + 0.4 \cdot \text{effort}$.

C. Cognitive Workload User Study

1) *Baseline conditions*: 2 baseline conditions. Each baseline condition corresponds to a fixed setting of $dist_t$ (either easy addition, or hard video transcription), without any robot query tasks.

2) *Sample study questions*: Below we provide examples of the robot queries that we ask in the online cognitive workload user study, covering each of the possible response types r_t and question difficulties d_t :

- $r_t = \text{MCQ}$, $d_t = \text{easy}$: “What kind of food item is outlined in the image below?” (Responses: “Raspberry”, “Strawberry”, “Grape”, “Apple”, “I don’t know.”)
- $r_t = \text{BB}$, $d_t = \text{easy}$: “Draw a box around only the strawberry.”
- $r_t = \text{OE}$, $d_t = \text{easy}$: “Why did the Robot fail in acquiring the cantaloupe?”
- $r_t = \text{MCQ}$, $d_t = \text{hard}$: “Which of the following images is tofu?” (Responses: “Left”, “Right”, “I don’t know.”)
- $r_t = \text{BB}$, $d_t = \text{hard}$: “Draw a box around only the carrot in the bottom right.”
- $r_t = \text{OE}$, $d_t = \text{hard}$: “How would you skewer the following item with a fork?”

3) *Compensation*: Users were compensated at a rate of \$12/hr, for a total compensation of \$18 for the entire study (as the study duration was 1.5 hr).

D. Cognitive Workload Predictive Models

1) *Discrete-time Models*: We consider different values of H , with one memoryless Granger model (where $H = 1$) and a set of Granger models with H ranging from 5 to 30. We chose the upper bound of $H = 30$ to roughly correspond to the study condition length in Section IV-A. This is because we set each discrete time step to correspond to 10s. For each of these models, we also consider variants where we imposed non-negativity constraints and/or ridge-regression penalties on the weights γ and \mathbf{w}_i^T . Specifically, we consider 4 different variants:

- Granger: no nonnegativity or ridge-regression penalty
- Granger-Nonnegative: nonnegativity constraint only
- Granger-Ridge: ridge-regression penalty only
- Granger-Ridge-Nonnegative: non-negativity constraint and ridge-regression penalty

2) *Continuous-time Models*: We also consider a continuous-time setting, where $CL(t)$ represents the cognitive workload at time t . In this setting, we consider one model (denoted as Exp-Impulse) that models the workload at the current time t as composed of a series of impulses at the query times, with an exponential decay in workload in between the queries. The Exp-Impulse model is defined recursively as follows:

$$CL(t) = CL(t_{prev})e^{-\lambda(t-t_{prev})} + \beta(d_t, r_t, dist_t)$$

where t_{prev} is the previous timestep at which we queried, $\beta(d_t, r_t, dist_t)$ is the magnitude of the impulse, and λ is the workload decay rate.

3) *Model Selection*: We consider a set of different linear models. For model selection, we perform 4-fold cross-validation on the full cognitive workload dataset D , consisting of $N = 4272$ unique question/workload pairs, where the performance measure for selecting a model is given by the predictive MSE on the held-out test split. For tuning of the ridge regression regularization parameter λ_r , we perform 5-fold cross validation to select the optimal parameter value, with a logarithmic range from 10^{-3} to 10^2 .

Table II shows the MSE statistics, computed across the 4 folds, for the set of learned models. Note that we also considered a constant baseline (denoted Constant), whose predicted workload is $CL_t = CL_0$, and an average baseline (denoted Average), whose predicted workload is the average value of CL_0 in the training set.

For the real-world user study in Section VI-B, we use a Granger model with $H = 5$, with a ridge-regression penalty on γ and \mathbf{w}_i^T , where the final selected ridge regression penalty was $\lambda_r = 10$. We use this model because it is the model with the lowest median test MSE. We initially considered using mean test MSE to select the best-performing model, but we discovered that the mean test MSE had a very large magnitude for certain models. This is because for the models that do not have weight constraints, linear regression learned parameters with large weight magnitudes (that overfit to the training set). Because of this, we use the median test MSE to select the model. Note that while the models have differences in their mean test MSE, the standard deviations in test MSE for the models overlap because of the variance across folds.

For the simulated experiments in Section VI-A, we use a Granger model with $H = 10$, where we place the following constraints on the parameters during model training: $\gamma, \{\mathbf{w}_i^T\}_{i=0}^{H-1} \in [0.5, 1]$, $w_0 \leq 1$.

E. Human-in-the-Loop Algorithms

We provide the full algorithmic description for LINUCB-EXPDECAY in Algorithm 2.

Model	H	Test MSE ($\mu \pm \sigma$)	Test MSE (median)
Constant	0	0.1271 ± 0.0173	0.1304
Average	0	0.0937 ± 0.0086	0.0922
Granger	1	0.0572 ± 0.0126	0.0507
	5	$7.59e+15 \pm 1.31e+16$	0.0656
	10	$3.16e+18 \pm 5.47e+18$	0.0661
	15	$1.87e+17 \pm 3.23e+17$	0.0660
	20	$5.41e+17 \pm 9.37e+17$	0.0663
	25	$1.39e+18 \pm 2.41e+18$	0.0668
	30	$1.09e+20 \pm 1.89e+20$	0.0677
Granger-Nonnegative	1	0.0573 ± 0.0126	0.0507
	5	0.0575 ± 0.0128	0.0508
	10	0.0575 ± 0.0128	0.0508
	15	0.0574 ± 0.0126	0.0508
	20	0.0575 ± 0.0127	0.0508
	25	0.0577 ± 0.0126	0.0508
	30	0.0578 ± 0.0125	0.0510
Granger-Ridge	1	0.0572 ± 0.0127	0.0507
	5	0.0573 ± 0.0127	0.0506
	10	0.0574 ± 0.0125	0.0509
	15	0.0574 ± 0.0124	0.0512
	20	0.0575 ± 0.0124	0.0512
	25	0.0579 ± 0.0123	0.0514
	30	0.0582 ± 0.0122	0.0515
Granger-Ridge-Nonnegative	1	0.0573 ± 0.0126	0.0508
	5	$5.66e+24 \pm 9.80e+24$	0.0655
	10	0.6120 ± 0.9559	0.0658
	15	0.0573 ± 0.0125	0.0508
	20	0.0574 ± 0.0125	0.0509
	25	0.1189 ± 0.1179	0.0514
	30	0.1195 ± 0.1021	0.0662
Exp-Impulse	-	0.0737 ± 0.0128	0.0678

TABLE II: Train and test mean-squared error (MSE) values for cognitive workload models.

Algorithm 2 LINUCB-EXPDECAY.

- 1: Inputs: Context x , decay rate c , number of food items seen N , time t
- 2: For all robot actions a_r , compute UCB bonus b_{a_r} and UCB value UCB_{a_r} .
- 3: Set $P(query) = e^{-cN}$ if t is the first timestep to observe x , $P(query) = 0$ otherwise.
- 4: Set $a = a_q$ with probability $P(query)$, $a = \arg \max_{a_r} UCB_{a_r}$ with probability $1 - P(query)$.
- 5: **return** a

F. Additional Results for Evaluation: Simulated Data

First, we include a set of additional metrics for the experimental setting described in Section VI-A, which focus on the observed convergence for each food item. We define the following metrics: $f_{q,food}$, which is the fraction of food items for which the algorithm queried; $f_{fail,food}$, which is the fraction of food items for which the algorithm was unable to converge; and $f_{auto,food}$, which is the fraction of food items for which the algorithm autonomously converged. Table III shows these metrics for $w_{task} = 0.4$.

Next, we include full results for multiple settings of w_{task} and w_{cl} , for the same cognitive workload model used in Section VI-A, ranging from $w_{task} \in \{0.2, 0.3, \dots, 0.9\}$, shown in Table IV. We see that LINUCB-QG performs the best for lower values of w_{task} (corresponding to a high-to-medium emphasis on minimizing workload), while ALWAYS-QUERY performs the best for higher values of w_{task} (corresponding to a high emphasis on maximum task

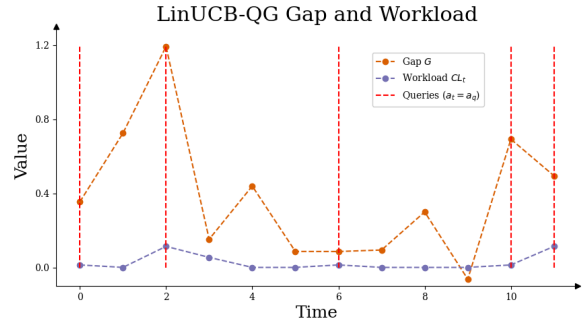


Fig. 5: Example LinUCB-QG rollout in simulation environment, illustrating evolution of performance gap G and workload CL_t , along with timesteps corresponding to query times. LinUCB-QG decides to ask the human for help when $G > wCL_t$ (in this rollout, $w = 4$).

performance, which the ALWAYS-QUERY baseline achieves due to its lack of exploration compared to LINUCB-QG).

Finally, Figure 5 shows a rollout of the workload model in simulation for LINUCB-QG, showing how the workload CL_t evolves over time, how the UCB estimate gap variable G varies, and when LINUCB-QG decides to query. In this example, LINUCB-QG decides to ask the human for help when $G > wCL_t$ (in this rollout, $w = 4$), but also recall that once LINUCB-QG has asked for help for the current food item, it will continue to execute the expert action until it has converged.

G. Feeding Tool

In our work, we use a custom feeding tool developed in prior work [9, 40], which is attached to the end of

Method	$f_{q,food}$	$f_{fail,food}$	$f_{auto,food}$
LINUCB	0 ± 0	0 ± 0	1 ± 0
ALWAYSQUERY	1 ± 0	0 ± 0	0 ± 0
LINUCB-EXPDECAY	0.4 ± 0.219	0.016 ± 0.054	0.584 ± 0.211
LINUCB-QG	0.76 ± 0.08	0 ± 0	0.24 ± 0.08

TABLE III: Additional convergence metrics in simulation on the test set, corresponding to $w_{task} = 0.4$. Averages are across 5 random seeds (For LINUCB-EXPDECAY, we also average across 5 policy random seeds).

w_{task}	Method	$r_{task,avg}$	ΔCL	M_{wt}	f_q	t_{conv}
0.2	LINUCB	0.289 ± 0.101	-0.5 ± 0	0.458 ± 0.020	-	3.92 ± 1.342
	ALWAYSQUERY	0.638 ± 0.189	-0.329 ± 0.106	0.391 ± 0.057	1 ± 0	1.68 ± 0.392
	LINUCB-EXPDECAY	0.368 ± 0.135	-0.496 ± 0.014	0.470 ± 0.024	0.4 ± 0.219	2.94 ± 0.894
	LINUCB-QG	0.407 ± 0.059	-0.5 ± 0	0.481 ± 0.012	0.76 ± 0.08	2.52 ± 0.449
0.3	LINUCB	0.289 ± 0.101	-0.5 ± 0	0.437 ± 0.030	-	3.92 ± 1.342
	ALWAYSQUERY	0.638 ± 0.189	-0.329 ± 0.106	0.422 ± 0.041	1 ± 0	1.68 ± 0.392
	LINUCB-EXPDECAY	0.368 ± 0.135	-0.496 ± 0.014	0.457 ± 0.037	0.4 ± 0.219	2.94 ± 0.894
	LINUCB-QG	0.407 ± 0.059	-0.5 ± 0	0.472 ± 0.018	0.76 ± 0.08	2.52 ± 0.449
0.5	LINUCB	0.289 ± 0.101	-0.5 ± 0	0.394 ± 0.051	-	3.92 ± 1.342
	ALWAYSQUERY	0.638 ± 0.189	-0.329 ± 0.106	0.484 ± 0.058	1 ± 0	1.68 ± 0.392
	LINUCB-EXPDECAY	0.368 ± 0.135	-0.496 ± 0.014	0.432 ± 0.064	0.4 ± 0.219	2.94 ± 0.894
	LINUCB-QG	0.407 ± 0.059	-0.5 ± 0	0.454 ± 0.030	0.76 ± 0.08	2.52 ± 0.449
0.6	LINUCB	0.289 ± 0.101	-0.5 ± 0	0.373 ± 0.061	-	3.92 ± 1.342
	ALWAYSQUERY	0.638 ± 0.189	-0.329 ± 0.106	0.515 ± 0.081	1 ± 0	1.68 ± 0.392
	LINUCB-EXPDECAY	0.368 ± 0.135	-0.496 ± 0.014	0.419 ± 0.078	0.4 ± 0.219	2.94 ± 0.894
	LINUCB-QG	0.407 ± 0.059	-0.5 ± 0	0.444 ± 0.035	0.76 ± 0.08	2.52 ± 0.449
0.7	LINUCB	0.289 ± 0.101	-0.5 ± 0	0.352 ± 0.071	-	3.92 ± 1.342
	ALWAYSQUERY	0.638 ± 0.189	-0.329 ± 0.106	0.545 ± 0.107	1 ± 0	1.68 ± 0.392
	LINUCB-EXPDECAY	0.368 ± 0.135	-0.496 ± 0.014	0.407 ± 0.092	0.4 ± 0.219	2.94 ± 0.894
	LINUCB-QG	0.407 ± 0.059	-0.5 ± 0	0.435 ± 0.041	0.76 ± 0.08	2.52 ± 0.449
0.8	LINUCB	0.289 ± 0.101	-0.5 ± 0	0.331 ± 0.081	-	3.92 ± 1.342
	ALWAYSQUERY	0.638 ± 0.189	-0.329 ± 0.106	0.576 ± 0.134	1 ± 0	1.68 ± 0.392
	LINUCB-EXPDECAY	0.368 ± 0.135	-0.496 ± 0.014	0.394 ± 0.106	0.4 ± 0.219	2.94 ± 0.894
	LINUCB-QG	0.407 ± 0.059	-0.5 ± 0	0.426 ± 0.047	0.76 ± 0.08	2.52 ± 0.449
0.9	LINUCB	0.289 ± 0.101	-0.5 ± 0	0.310 ± 0.091	-	3.92 ± 1.342
	ALWAYSQUERY	0.638 ± 0.189	-0.329 ± 0.106	0.607 ± 0.161	1 ± 0	1.68 ± 0.392
	LINUCB-EXPDECAY	0.449 ± 0.157	-0.468 ± 0.042	0.451 ± 0.139	0.72 ± 0.098	2.536 ± 0.941
	LINUCB-QG	0.407 ± 0.059	-0.5 ± 0	0.417 ± 0.053	0.76 ± 0.08	2.52 ± 0.449

TABLE IV: Querying bandit algorithm metrics in simulation on the test set for different values of w_{task} . Averages are across 5 random seeds (For LINUCB-EXPDECAY, we also average across 5 policy random seeds). Values for $r_{task,avg}$ and r_{CL} correspond to the hyperparameter setting with maximal M_{wt} on the validation set.

the Kinova’s Robotiq 2F-85 gripper. The tool consists of a motorized fork with two degrees of freedom: pitch β and roll γ . Each of the six robot actions a_r (for $r \in \{1, \dots, 6\}$) corresponds to a unique value of β and γ . In particular, the pitch configuration (either TA, VS, or TV) affects the value of β , while the roll configuration (either 0° or 90°) affects the value of γ .

H. Additional Results for Evaluation: Real-world User Study

Pre-method questions. We ask the user the following questions prior to each method:

- “How mentally burdened do you feel currently?”
- “How hurried or rushed do you feel currently?”

Post-method questions. We ask the user the following questions after each method:

- “For the last method, how mentally burdened do you feel currently because of the robot querying you?”
- “For the last method, how hurried or rushed do you feel currently because of the robot querying you?”
- “For the last method, how hard did you have to work to make the robot feed you?”
- “For the last method, how successful was the robot in picking up the food item and bringing it to your mouth?”

Compensation. Users were compensated at a rate of \$12/hr, for a total compensation of \$18 for the entire study (as the study duration was 1.5 hr).

Method comparison across all metrics. Tables V and VI include comparisons across the three methods used in the real-world user study (LINUCB, ALWAYSQUERY, LINUCB-QG) for the 7 subjective and 3 objective metrics mentioned in Section VI-B, respectively. For all metrics, we find that LINUCB-QG achieves an intermediate value for that metric compared to the other two algorithms, suggesting that our method finds a balance between cognitive workload and task performance (which these metrics cover). Additionally, Table VII shows the full results of the Wilcoxon paired signed-rank tests that we used to determine whether LINUCB-QG exhibited statistically significant differences in the full set of metrics compared to LINUCB-QG and ALWAYSQUERY. For the metrics related to cognitive workload, our alternative hypothesis was that the value of the metric for LINUCB-QG was less than the value for ALWAYSQUERY. For the metrics related to task performance, our alternative hypothesis was that the value of the metric for LINUCB-QG was greater than the value for LINUCB. For all metrics, we find that LINUCB-QG has a statistically significant

improvement compared to the baseline for that metric.

Comments on Post-Performance metric. When looking at the Post-Performance metric, we find that LINUCB-QG achieves an intermediate value, higher than LINUCB but lower than ALWAYS-QUERY. When asking users to rate subjective success, we asked them to rate the overall success of each algorithm, which depends on both whether the algorithm successfully picked up food items and how many attempts were required for success. For this reason, we believe that users rated the success of ALWAYS-QUERY highly because it efficiently selects the optimal action for each food item within one timestep, whereas LINUCB-QG sometimes takes multiple timesteps if it does not query for a particular food item.

ACKNOWLEDGMENT

This work was partly funded by NSF CCF 2312774 and NSF OAC-2311521, a LinkedIn Research Award, and a gift from Wayfair, and by NSF IIS 2132846 and CAREER 2238792. The authors would like to thank Ethan Gordon for his assistance with the food dataset, Pranav Thakkar and Rishabh Madan for their help with running the robot user study, Janna Lin for providing the voice interface, and all of the participants in our two user studies.

Method	Post-Mental	Post-Temporal	Post-Performance	Post-Effort	Delta-Mental	Delta-Temporal	Delta-Weighted TLX
LINUCB	1.25 ± 0.60	1.39 ± 0.99	3.06 ± 0.78	1.25 ± 0.77	-0.36 ± 0.90	-0.28 ± 0.94	-0.025 ± 0.17
ALWAYSQUERY	3.14 ± 1.33	2.67 ± 1.55	4.65 ± 0.73	3.14 ± 1.27	1.5 ± 1.38	0.92 ± 1.79	0.41 ± 0.31
LINUCB-QG	2.33 ± 1.10	2.14 ± 1.22	4.06 ± 1.04	2.31 ± 1.04	0.67 ± 1.07	0.39 ± 1.10	0.22 ± 0.20

TABLE V: Subjective metric results for the real-world user study.

Method	$r_{task,avg}$	$n_{success}$	n_q
LINUCB	0.375 ± 0.086	2.0 ± 0.236	—
ALWAYSQUERY	0.862 ± 0.253	2.667 ± 0.624	3 ± 0
LINUCB-QG	0.682 ± 0.284	2.528 ± 0.726	1.722 ± 0.768

TABLE VI: Objective metric results for the real-world user study.

Metric	Hypothesis	p
Post-Mental	LINUCB-QG < ALWAYSQUERY	$3.28e-4$
Post-Temporal		$1.42e-2$
Post-Effort		$1.2e-4$
Delta-Mental		$7.68e-4$
Delta-Temporal		$1.82e-2$
Delta-Weighted TLX		$1.47e-4$
n_q		0
Post-Performance	LINUCB-QG > LINUCB	$2.68e-4$
$r_{task,avg}$		$2.66e-4$
$n_{success}$		$3.44e-4$

TABLE VII: Wilcoxon paired signed-rank test results for the real-world user study, showing p -values associated with cognitive load metrics (top) and task performance metrics (bottom). For all tests, we used a significance level of $\alpha = 0.05$.